Micromechanics of hybrid composite laminate with natural and synthetic fibres

MICROMECHANICS OF HYBRID COMPOSITE LAMINA WITH NATURAL AND SYNTHETIC FIBRES

Nenglong Yang[1], Zhenmin Zou[1], Prasad Potluri[2, 3] and Kali Babu Katnam[1, 2] *

[1] Department of Mechanical, Aerospace and Civil Engineering, The University of Manchester, UK
[2] Northwest Composites Centre, The University of Manchester, UK
[3] Department of Materials, The University of Manchester, UK
* Corresponding author (Kali-Babu.Katnam@manchester.ac.uk)

Keywords: Fibre hybrid composites, RVE modelling, Homogenisation, Micro-stress fields

ABSTRACT

This study investigates the effect of intra-laminar fibre hybridisation on the homogenised lamina properties and micro-stress fields, with an emphasis on natural and synthetic fibre combinations. A representative volume element (RVE) approach, considering random fibre distributions, is employed to study unidirectional flax/E-glass/epoxy composite laminae. The results indicate that intra-laminar hybridisation with natural and synthetic fibre combinations can offer opportunities to tailor the homogenised lamina properties, especially to vary the effective density and thus achieve high specific properties. In addition, it is shown that the intra-laminar hybridisation can significantly alter the micro-stress and strain fields, potentially affecting intra-laminar damage mechanisms.

1 INTRODUCTION

In recent years, the growing awareness of environmental protection and sustainability has motivated the use of natural fibres as reinforcements in fibre-reinforced polymer materials to replace synthetic fibres. The rising market demand for more sustainable, recyclable and biodegradable materials is expected to continue in the coming years [1]. Natural fibre-reinforced composites (NFRCs) are being increasingly used in secondary structural applications, such as in automotive components (e.g., door panels, dashboards and seats), construction materials (e.g., pipes, wall and roof panels) and sports equipment (e.g., bicycle racks, tennis rackets and golf clubs) [2, 3]. The market growth of NFRCs is attributed to their desirable factors, such as high specific strength and stiffness, low cost and production energy, non-toxicity and biodegradability. However, NFRCs have certain disadvantages, such as low durability, high moisture absorption, low thermal stability, variation in mechanical properties and dimensional instability, which could significantly influence the structural integrity and reliability of NFRC-based structural components and thus are major hurdles to their use in primary structural applications. To address some of these limitations, natural and synthetic fibres can be combined to produce natural fibre-based hybrid composites (NFHCs), such as inter-laminar (with different single fibre-based laminae) or intra-laminar (with more than one fibre-based laminae) hybrid laminate [4].

Many experimental studies have been conducted to investigate the mechanical behaviour of NFHCs [5-16]. In these studies, E-glass fibres are the most commonly used synthetic fibres added to NFRCs. For instance, flax [5, 6], hemp [7, 8], sisal [9, 10], basalt [11-13] and jute [14, 15] have all been hybridised with E-glass fibres. Zhang et al. [5] experimentally investigated the effect of fibre volume fraction and inter-laminar hybridisation on the tensile properties of unidirectional flax/E-glass composites and showed that the tensile strength and failure strain of laminates can be improved with increased E-glass fibre content, but with no considerable effect on the tensile modulus. Moreover, the interlaminar shear strength and fracture toughness were enhanced with inter-laminar hybridisation. In the experimental study of hemp/E-glass composites, Prashanth et al. [15] reported that the inter-laminar hybridisation of hemp fibre-based laminates with E-glass fibres resulted in enhancing the mechanical properties (tensile, flexural and impact responses) when compared to those of the hemp FRCs. Similarly, Abd El-baky et al. [16] reported that increasing the E-glass fibre content improved the mechanical properties of flax/E-glass composites. Experimental studies on the inter-laminar hybridisation of basalt fibre-based laminates with E-glass fibres [11-13] showed that the addition of E-glass fibres to basalt composites decreases the overall density as well as the tensile and flexural moduli of the laminates.

Furthermore, the impact strength of basalt/E-glass laminates was found to be higher than that of both basalt fibre-based and E-glass fibre-based laminates [12]. The literature thus indicates that NFHCs can potentially replace conventional composites with synergistic effects on the mechanical properties of laminates, and that these material properties are significantly influenced by a range of factors, including fibre and matrix types, fibre volume fractions, fibre orientation, stacking sequence, and matrix-fibre interfacial adhesion.

Although several experimental studies in the literature have reported on the inter-laminar hybridisation of natural fibre-based laminates with synthetic fibres, no studies have been conducted on intra-laminar hybridisation [17]. A few experimental studies have investigated the intra-laminar hybridisation of synthetic fibre-based laminates [18-20]. Moreover, several computational studies have investigated the mechanical behaviour of synthetic/synthetic fibre hybrid composite laminates, such as the inter-laminar hybridisation of Kevlar fibre-based laminates with E-glass [21], carbon fibre-based woven laminates with Dyneema [22], carbon fibre-based laminates with Kevlar [23], and on the intra-laminar hybridisation of carbon fibre-based laminae with E-glass [24, 25]. These studies have mostly been based on the computational micromechanics of composites using representative volume element (RVE) models [26] with periodic boundary conditions [27]. However, no computational studies have been reported on the intra-laminar hybridisation of natural fibre-based laminates. In this regard, a computational study has been conducted to focus on the intra-laminar hybridisation of natural fibre-based laminae with synthetic fibres to understand the effect of fibre hybridisation on the homogenised lamina properties as well as intra-laminar micro-stress fields. A RVE model has been developed in the current study to investigate flax/E-glass intra-laminar hybrid composite laminae and implemented using Python and ABAQUS/Standard.

2 MICROMECHANICAL RVE MODEL

A 3D RVE model is developed for fibre hybrid unidirectional laminae. In this model, both the synthetic fibres and matrix within the lamina are considered to be continuous, homogeneous, isotropic and defect-free. However, the natural fibres are considered to be transversely isotropic. Additionally, the fibres are assumed to possess circular cross-sections. A perfect matrix-fibre interface is also assumed for both fibre types. Considering a random fibre distribution within the hybrid lamina, the microstructure of the RVE is generated using the random sequential expansion (RSE) algorithm [28]. The RSE algorithm is modified to populate both synthetic and natural fibres and achieve target fibre volume fractions. The modified algorithm ensures that the large fibres are placed first within the RVE domain, creating enough space to accommodate the small fibres and reaching the targeted volume fractions for both fibre types. The modified algorithm also ensures geometric periodicity at the boundaries of the RVE (i.e., when a fibre contacts the boundary of the model, the portion of the fibre beyond the boundary is also placed on the opposite boundary) to apply period boundary conditions. In the current study, the RVE model is applied to study unidirectional flax/E-glass/epoxy hybrid composite laminae. Considering that the total fibre volume fraction is fixed at 0.6, the individual fibre volume fractions are varied and different microstructures are generated. Representative microstructure for each combination of fibre volume fractions for the flax/E-glass/epoxy lamina are shown in Fig. 1, where the flax fibre volume fraction, the E-glass fibre volume fraction and the matrix volume fraction are denoted by V_{fF}, V_{fE} and V_m, respectively.

Using Python and ABAQUS/Standard, the RVE model is implemented within the framework of the finite element method. The micro-stress/strain fields and the homogenised material properties are obtained by imposing displacement-based periodic boundary conditions. The material properties and the fibre diameters used in the RVE models are given in Table 1. The RVE size is selected by considering the large fibre diameter as the characteristic length of the micro-constituents. To ensure that the RVE is sufficiently large compared to the fibre diameters, the length and width of the RVE (the dimensions perpendicular to the fibre direction) are 15 times the diameter of the large fibre. For the flax-/E-glass/epoxy hybrid lamina, as the flax fibres are assumed to be circular with a diameter of 30 μm, the length (and width) of the RVE used is 450 μm. Because of the unidirectional fibres, a small value (of the order of the radius of the small fibre) is used for the thickness

of the RVE (along the fibre direction). The matrix and the fibres are modelled using C3D8R and C3D6 elements, respectively. A mesh convergence study is conducted to determine the average element size of the RVE. An element size of 1/8 of the radius of the small fibre (i.e., ~0.9375 μm for the flax/E-glass/epoxy lamina) is used to mesh the RVEs, with only one element along the thickness direction.

Table 1: The properties of the constituents [4, 29-34] and the fibre diameters used in the RVEs.

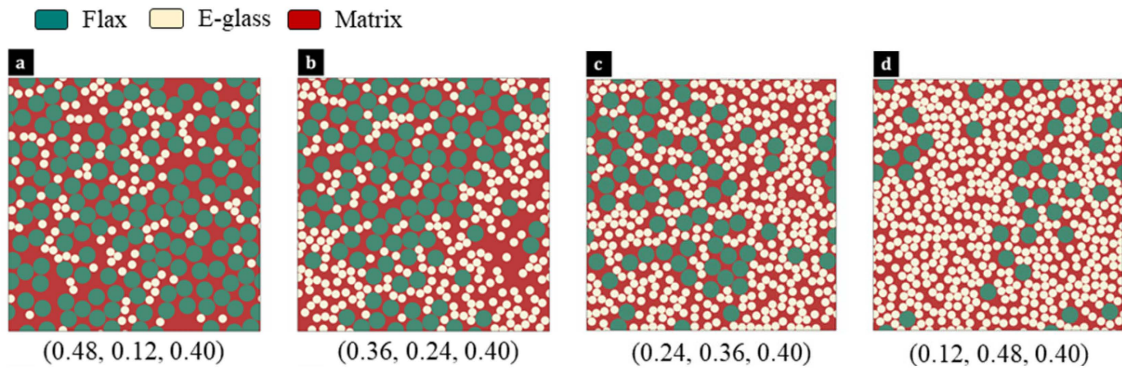| Constituent	E_1 (GPa)	E_2 (GPa)	G_{12} (GPa)	G_{23} (GPa)	ν_{12}	ν_{23}	Density (g/cm^3)	Diameter (μm)
E-glass	73	73	30.4	30.4	0.2	0.2	2.5	15
Flax	54.1	7	3	2	0.3	0.75	$1.4 - 1.5$	30
Epoxy	2.55	2.55	0.94	0.94	0.35	0.35	1.15	-

Figure 1: Representative microstructures generated by using the modified RSE algorithm for the RVE model of the flax/E-glass/epoxy lamina with different fibre volume fractions (V_{fF}, V_{fE}, V_m): (a) (0.48, 0.12, 0.40), (b) (0.36, 0.24, 0.40), (c) (0.24, 0.36, 0.40), and (d) (0.12, 0.48, 0.40).

The RVE model is used, and the homogenised lamina properties are obtained by volume averaging the micro-stress fields using the procedure in Li and Sitnikova [35]. This procedure employs six key degrees of freedom (kdofs) to impose the macro-stress state (with six independent components). Using the kdofs, which are implemented in ABAQUS with six reference nodes, six loading cases are considered (i.e., three normal and three shear loading cases). The reference nodes are used to apply generalised forces (which are related to the volume average of the microscopic stress components or the macroscopic stress components) or generalised displacements (which are related to the volume average of the microscopic strain components or the macroscopic strain components) [35]. Either the generalised nodal forces are applied to obtain the generalised nodal displacements or the generalised nodal displacements are applied to obtain the generalised nodal forces. When the generalised nodal forces are applied to the RVE, the homogenisation procedure with the six loading cases provides the compliance matrix, which can be used to obtain the homogenised engineering constants for the hybrid lamina. The generalised nodal displacements at each reference point are proportional to the six macroscopic strain components $(\hat{\varepsilon}_{11}, \hat{\varepsilon}_{22}, \hat{\varepsilon}_{33}, \hat{\varepsilon}_{12}, \hat{\varepsilon}_{13}, \hat{\varepsilon}_{23})$, which are connected to the periodic boundary conditions. The subscripts 1, 2 and 3 are associated with the material principal directions, i.e., the longitudinal and transverse directions. Similarly, the generalised nodal forces at each reference point are proportional to the six macroscopic stress components $(\hat{\sigma}_{11}, \hat{\sigma}_{22}, \hat{\sigma}_{33}, \hat{\sigma}_{12}, \hat{\sigma}_{13}, \hat{\sigma}_{23})$. In this study, six generalised forces are individually applied, representing the six loading cases, and the corresponding generalised displacements and then the compliance matrix are obtained from the RVE models. The generalised forces $(F_{11}, F_{22}, F_{33}, F_{12}, F_{13}, F_{23})$ at the reference points are linked to the six macroscopic stresses $(\hat{\sigma}_{11}, \hat{\sigma}_{22}, \hat{\sigma}_{33}, \hat{\sigma}_{12}, \hat{\sigma}_{13}, \hat{\sigma}_{23})$ and the volume of the RVE (Ω) via energy equivalence [35] as in Eq. 1.

$$F_{ij} = \hat{\sigma}_{ij}\Omega \qquad (i, j = 1, 2, 3) \tag{1}$$

To determine the homogenised lamina properties, the six loading cases are analysed individually (i.e., for each macroscopic stress component) using the RVE model. For the first loading case, the generalised force F_{11} is applied only, with a magnitude equal to the volume of the RVE, i.e., Ω. From Eq. 1, it represents the uni-axial tensile loading case with the corresponding macroscopic stress component, $\hat{\sigma}_{11} = 1$. Using the corresponding generalised displacement, the homogenised properties ($\hat{E}_{11}, \hat{v}_{12}, \hat{v}_{13}$) can then be obtained using Eq. 2 [35]. The remaining homogenised properties are obtained similarly for the other loading cases, and the complete set of homogenised properties ($\hat{E}_{11}, \hat{E}_{22}, \hat{E}_{33}, \hat{G}_{12}, \hat{G}_{13}, \hat{G}_{23}, \hat{v}_{12}, \hat{v}_{13}, \hat{v}_{23}$) can be determined.

$$\hat{E}_{11} = \frac{\hat{\sigma}_{11}}{\hat{\varepsilon}_{11}} = \frac{1}{\hat{\varepsilon}_{11}}; \quad \hat{v}_{12} = -\frac{\hat{\varepsilon}_{22}}{\hat{\varepsilon}_{11}}; \quad \hat{v}_{13} = -\frac{\hat{\varepsilon}_{33}}{\hat{\varepsilon}_{11}} \tag{2}$$

3 MECHANICAL BEHAVIOUR OF FIBRE HYBRID COMPOSITE LAMINA

The RVE modelling approach and the homogenisation procedure presented in Sec. 2 are applied to the flax/E-glass/epoxy laminae with different fibre volume fractions. In addition, flax/epoxy and E-glass/epoxy laminae are also analysed to validate the RVE model with analytical models applicable to non-hybrid unidirectional laminae (with only one fibre type as the reinforcing constituent) for estimating the homogenised lamina properties. A sanity check, as described by Li and Sitnikova [35], is initially performed by assigning the material properties of the fibre to be the same as the matrix and analysing the RVE for the six independent loading conditions. The sanity check is done to verify whether the model can produce the desired output in the simplest case [35], including the imposed periodic boundary and loading conditions.

3.1 Hybrid lamina: Homogenised properties

To validate the RVE model, non-hybrid unidirectional laminae, i.e., E-glass/epoxy and flax/epoxy unidirectional laminae, are first analysed, considering a fibre volume fraction of 0.6. Five different microstructures are analysed, and the average homogenised properties are obtained. The average homogenised lamina properties of E-glass/epoxy are given in Table 2 and are compared with the analytical estimations obtained using the Chamis, Halpin-Tsai and Mori-Tanaka models [36-38]. Similarly, the average homogenised properties of flax/epoxy unidirectional lamina are given in Table 3. The comparison shows that a good agreement for the longitudinal modulus ($\hat{E}_{11}$) and the major Poisson's ratio ($\hat{v}_{12}$), while a considerable error for the other properties. In comparison with the RVE data, the Chamis equations [36] are found to predict the homogenised properties of the E-glass/epoxy lamina with low relative error, while the Halpin-Tsai equations [37] are seen to be the more accurate in predicting the properties of the flax/epoxy lamina. Overall, the comparisons in Tables 2 and 3 validate the RVE model. The standard deviation of the homogenised properties obtained from the RVE models shows that the homogenised properties are not dependent on the microstructure, thus, the size of the RVE used is appropriate.

Table 2: The comparison of the homogenised properties of E-glass/epoxy unidirectional lamina (with a fibre volume fraction of 0.6) obtained from the RVE model and the Chamis, Halpin-Tsai and Mori-Tanaka analytical models.

	RVE	Chamis [36]		Halpin-Tsai [37]		Mori-Tanaka [38]	
		Estimation	Error %	Estimation	Error %	Estimation	Error %
$\hat{E}_{11}$ (GPa)	44.76 ± 0.02	44.82	0.1	44.82	0.1	44.84	0.2
$\hat{v}_{12}$	0.25 ± 0.00	0.26	3.9	0.26	3.9	0.25	0.0
$\hat{E}_{22}$ (GPa)	10.70 ± 0.23	10.10	5.8	12.14	12.6	7.58	34.1
$\hat{G}_{12}$ (GPa)	4.24 ± 0.05	3.79	11.2	3.64	15.2	3.39	22.3
$\hat{G}_{23}$ (GPa)	3.95 ± 0.08	3.79	4.1	3.64	8.2	2.98	28.0

Table 3: The comparison of the homogenised properties of flax/epoxy unidirectional lamina (with a fibre volume fraction of 0.6) obtained from the RVE model and the Chamis, Halpin-Tsai and Mori-Tanaka analytical models.

	RVE	Chamis [36]		Halpin-Tsai [37]		Mori-Tanaka [38]	
		Estimation	Error %	Estimation	Error %	Estimation	Error %
$\hat{E}_{11}$ (GPa)	33.44 ± 0.04	33.48	0.1	33.48	0.1	33.48	0.1
$\hat{v}_{12}$	0.32 ± 0.01	0.32	0.0	0.32	0.0	0.32	0.0
$\hat{E}_{22}$ (GPa)	4.79 ± 0.23	5.02	4.7	4.75	0.8	4.02	17.5
$\hat{G}_{12}$ (GPa)	1.83 ± 0.00	2.01	9.4	1.83	0.0	1.80	1.7
$\hat{G}_{23}$ (GPa)	1.51 ± 0.13	1.60	5.8	1.47	2.7	1.44	4.7

The average homogenised properties of the flax/E-glass/epoxy lamina are obtained from five different microstructures for each combination of fibre volume fractions and presented in Table 4. It can be seen that the homogenised properties of the flax/E-glass laminae with different hybrid volume fractions within the homogenised properties of the flax/epoxy lamina (lower bound) and the E-glass/epoxy lamina (upper bound) as expected. It is observed that the longitudinal modulus ($\hat{E}_{11}$) of the flax/E-glass/epoxy lamina decreases with higher flax fibre volume content. A similar trend is observed for the transverse modulus ($\hat{E}_{22}$), the in-plane and transverse shear moduli ($\hat{G}_{12}$ and $\hat{G}_{23}$) and the major Poisson's ratio ($\hat{v}_{12}$). To account for the effect of the increasing volume fraction of low density flax fibres on the effective density ($\hat{\rho}$) of the flax/E-glass/epoxy, the homogenised specific properties are obtained and given in Table 5. The specific longitudinal modulus ($\hat{E}_{11}$) and the major Poisson's ratio ($\hat{v}_{12}$) of the flax/E-glass/epoxy lamina are increased with higher flax fibre volume content.

Table 4: The homogenised properties for the flax/E-glass/epoxy lamina with varying flax and E-glass fibre volume fractions (and with a total fibre volume fraction of 0.6).

(V_{fF}, V_{fE}, V_m)	$\hat{E}_{11}$ (GPa)	$\hat{v}_{12}$	$\hat{E}_{22}$ (GPa)	$\hat{G}_{12}$ (GPa)	$\hat{G}_{23}$ (GPa)	$\hat{\rho}$ (g/cm^3)
(0.60, 0.00, 0.40)	33.44 ± 0.04	0.32 ± 0.02	4.79 ± 0.23	1.83 ± 0.00	1.51 ± 0.13	1.33
(0.48, 0.12, 0.40)	35.84 ± 0.00	0.30 ± 0.00	5.40 ± 0.01	2.13 ± 0.01	1.70 ± 0.00	1.46
(0.36, 0.24, 0.40)	37.95 ± 0.00	0.29 ± 0.00	6.28 ± 0.08	2.49 ± 0.03	2.02 ± 0.02	1.58
(0.24, 0.36, 0.40)	40.31 ± 0.00	0.27 ± 0.00	7.47 ± 0.11	2.95 ± 0.03	2.45 ± 0.02	1.71
(0.12, 0.48, 0.40)	42.42 ± 0.00	0.26 ± 0.00	8.91 ± 0.06	3.54 ± 0.03	3.05 ± 0.04	1.83
(0.00, 0.60, 0.40)	44.76 ± 0.02	0.25 ± 0.00	10.7 ± 0.22	4.24 ± 0.05	3.95 ± 0.08	1.96

Table 5: The specific homogenised properties of the flax/E-glass/epoxy lamina with varying flax and E-glass fibre volume fractions (and with a total fibre volume fraction of 0.6).

(V_{fF}, V_{fE}, V_m)	$\hat{E}_{11}/\hat{\rho}$ (GPa. cm^3/g)	$\hat{v}_{12}/\hat{\rho}$ (cm^3/g)	$\hat{E}_{22}/\hat{\rho}$ (GPa. cm^3/g)	$\hat{G}_{12}/\hat{\rho}$ (GPa. cm^3/g)	$\hat{G}_{23}/\hat{\rho}$ (GPa. cm^3/g)
(0.60, 0.00, 0.40)	25.14	0.24	3.60	1.38	1.14
(0.48, 0.12, 0.40)	24.62	0.21	3.71	1.46	1.17
(0.36, 0.24, 0.40)	23.99	0.18	3.97	1.57	1.28
(0.24, 0.36, 0.40)	23.60	0.16	4.37	1.73	1.43
(0.12, 0.48, 0.40)	23.13	0.14	4.86	1.93	1.66
(0.00, 0.60, 0.40)	22.84	0.13	5.46	2.16	2.02

3.2 Micro-stress fields: The effect of fibre hybridisation

To show the effect of fibre hybridisation on the intra-laminar matrix stresses, the von Mises stress distribution within the matrix is presented in Figs. 2-3. In Fig. 2, the von Mises stress distribution is normalised and shown for the flax/epoxy lamina, with $(V_{fF}, V_{fE}, V_m) = (0.60, 0.0, 0.40)$, for the six loading conditions (i.e., unit macro stress components, i.e., $\hat{\sigma}_{ij} = 1$ MPa). As can be seen in Figs. 2a-2f, where the fibres are removed, and only the matrix is shown, the von Mises matrix stress amplification is induced under the two in-plane shear loading cases (3.65 MPa and 3.80 MPa under $\hat{\sigma}_{12}$ and $\hat{\sigma}_{13}$, respectively), while the highest matrix stress amplification is observed under the transverse shear loading (5.04 MPa under $\hat{\sigma}_{23}$). Similarly, the von Mises matrix stress amplifications are shown in Figs. 3a-3f for the six loading cases for the flax/E-glass/epoxy lamina with $(V_{fF}, V_{fE}, V_m) = (0.48, 0.12, 0.40)$. In comparison with the von Mises matrix stress amplification in the flax/epoxy lamina, with an E-glass fibre volume fraction of 0.12, the von Mises matrix stress amplification is considerably higher under the two in-plane shear loading cases (14.24 MPa and 15.04 MPa under $\hat{\sigma}_{12}$ and $\hat{\sigma}_{13}$, respectively), which are higher than the matrix stress amplification obtained under the transverse shear loading (7.96 MPa under $\hat{\sigma}_{23}$). Similarly, under the transverse tensile loading cases ($\hat{\sigma}_{22}$), the von Mises matrix stress amplification is ~2.05 MPa for the flax/epoxy lamina, while it is considerably higher (4.09 MPa) for the flax/E-glass/epoxy lamina (see Figs. 2b and 3b). These von Mises matrix stress distributions indicate that the combination of the fibre volume fractions influences the intra-laminar micro-stress fields. As the modulus of E-glass fibres is higher than that of the flax fibres, the stress amplifications induced are higher with increasing E-glass fibre content, and such localised stress concentrations could thus influence intra-laminar damage mechanisms.
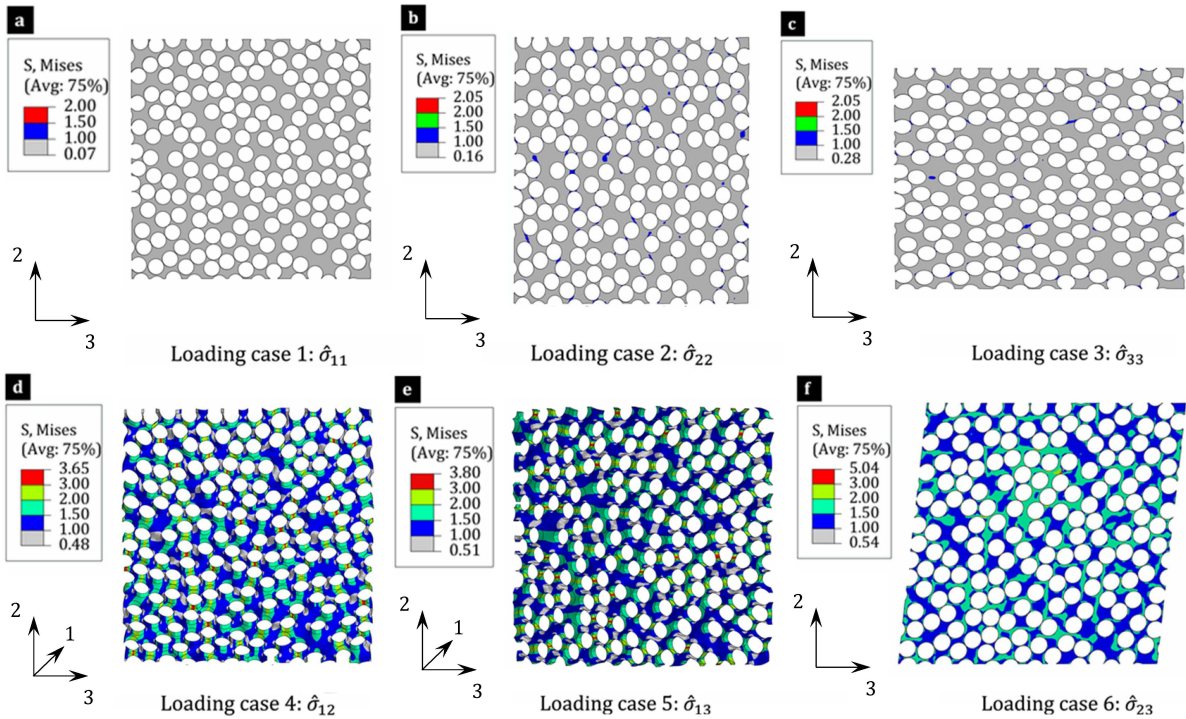

Figure 2: The von Mises stress fields in the matrix of the flax/epoxy lamina with $(V_{fF}, V_{fE}, V_m) = (0.60, 0.0, 0.40)$ under the six independent loading cases (the unit macro-stress components, in MPa): (a) $\hat{\sigma}_{11} = 1$, (b) $\hat{\sigma}_{22} = 1$, (c) $\hat{\sigma}_{33} = 1$, (d) $\hat{\sigma}_{12} = 1$, (e) $\hat{\sigma}_{13} = 1$, and (f) $\hat{\sigma}_{23} = 1$.
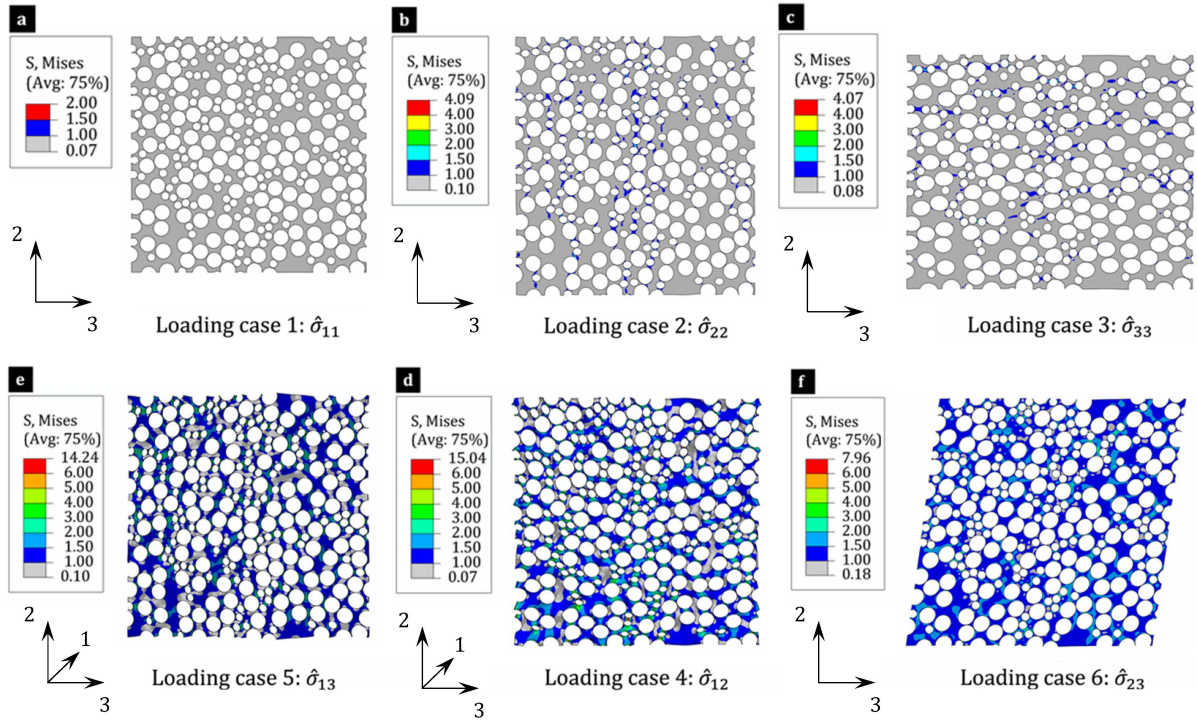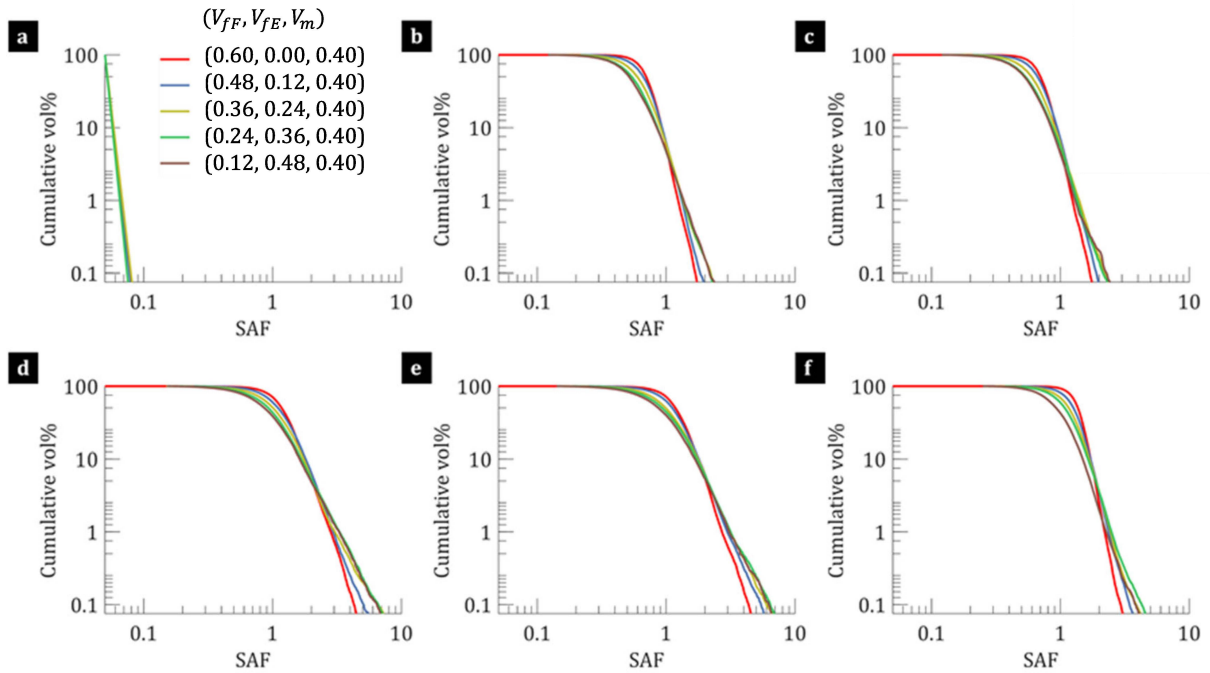
Figure 3: The von Mises stress fields in the matrix of the flax/E-glass/epoxy lamina with $\left(V_{fF}, V_{fE}, V_m\right) = (0.48, 0.12, 0.40)$ under the six independent loading cases (the unit macro-stress components, in MPa): (a) $\hat{\sigma}_{11} = 1$, (b) $\hat{\sigma}_{22} = 1$, (c) $\hat{\sigma}_{33} = 1$, (d) $\hat{\sigma}_{12} = 1$, (e) $\hat{\sigma}_{13} = 1$, and (f) $\hat{\sigma}_{23} = 1$.

Figure 4: The reversed cumulative volume % of the matrix versus the von Mises stress amplification factor (SAF) for the flax/E-glass/epoxy lamina with varying fibre volume fractions under the six loading cases: (a) $\hat{\sigma}_{11} = 1$, (b) $\hat{\sigma}_{22} = 1$, (c) $\hat{\sigma}_{33} = 1$, (d) $\hat{\sigma}_{12} = 1$, (e) $\hat{\sigma}_{13} = 1$, and (f) $\hat{\sigma}_{23} = 1$.

Using the RVEs, the effect of the microstructure on the von Mises matrix stress amplification factor (SAF) of flax/E-glass laminae is further investigated. For each combination of fibre volume fractions, the micro-stress fields are obtained considering five different microstructures. As a sufficiently large RVE size is used, the variation in the microstructure is observed to have a negligible effect on the RVE response. For the flax/E-glass/epoxy laminae, each combination of fibre volume fractions is considered, and the reversed cumulative distribution plots are obtained by using the matrix volume percentage and SAF. For the six loading cases, the reversed cumulative distribution data are shown in Fig. 4, with five different combinations of fibre volume fractions. It can be seen that the reversed cumulative distributions are sensitive to the fibre volume fraction of E-glass fibres as higher SAFs are induced with increasing E-glass fibre content. As shown in Fig. 4a, under the longitudinal tensile loading case, the reverse cumulative distribution is insensitive to the E-glass fibre volume fraction. In contrast, for the other five loadings (transverse tensile, in-plane shear and transverse shear) conditions, the matrix stress distribution is considerably influenced by the E-glass fibre content. In general, this suggests that the fibre content of synthetic fibres (with relatively high modulus) can alter matrix stress distributions, which can also affect fibre-matrix interface shear and normal stresses in fibre hybrid laminae with natural and synthetic fibres.

4 CONCLUSIONS

In this work, a representative volume element (RVE) model is developed for hybrid unidirectional lamina with natural and synthetic fibres. The microstructure of the RVEs are generated using a modified RSE algorithm. The RVE model is employed to investigate the homogenised lamina properties of and the micro-stress fields in the flax/E-glass/epoxy hybrid laminae with different combinations of fibre volume fractions. The RVE model has been validated against existing analytical models by comparing the homogenised lamina properties. The results show that the intra-laminar fibre hybridisation of the E-glass/epoxy lamina with flax fibres can be used to alter the homogenised properties. With an increasing flax fibre content, the effective density can be varied, and thus the specific lamina properties be tailored. Moreover, the von Mises matrix stress fields show that the matrix stress concentrations in the flax/epoxy lamina are relatively lower compared to the flax/E-glass/epoxy hybrid lamina, and the matrix stress concentrations are increased with increasing E-glass fibre content. In general, the developed RVE can be employed to study intra-laminar fibre hybrid laminae with natural and synthetic fibres, and the effect of such fibre hybridisation can be analysed to tailor hybrid composites and achieve desirable properties.

REFERENCES

[1] R. Fangueiro and S. Rana, Advances in Natural Fibre Composites : Raw Materials, Processing and Analysis, *3rd International Conference on Natural Fibers (Eds. R. Fangueiro and S. Rana)*, *Cham, Switzerland*, *June 21-23 2018*, Springer International Publishing.

[2] G. Kretsis, A review of the tensile, compressive, flexural and shear properties of hybrid fibre-reinforced plastics, *Composites*, **18**, 1987, pp. 13-23, (doi: 10.1016/0010-4361(87)90003-6).

[3] A. Lotfi, H. Li, D.V. Dao, and G. Prusty, Natural fiber–reinforced composites: A review on material, manufacturing, and machinability, *Journal of Thermoplastic Composite Materials*, **34**, 2019, pp. 238-284, (doi: 10.1177/0892705719844546).

[4] Y. Swolfs, I. Verpoest, and L. Gorbatikh, Recent advances in fibre-hybrid composites: materials selection, opportunities and applications, *International Materials Reviews*, **64**, 2019, pp. 181-215, (doi: 10.1080/09506608.2018.1467365).

[5] Y. Zhang, Y. Li, H. Ma, and T. Yu, Tensile and interfacial properties of unidirectional flax/glass fiber reinforced hybrid composites, *Composites Science and Technology*, **88**, 2013, pp. 172-177, (doi: 10.1016/j.compscitech.2013.08.037).

[6]   M. Cihan, A.J. Sobey, and J.I.R. Blake, Mechanical and dynamic performance of woven flax/E-glass hybrid composites, *Composites Science and Technology*, **172**, 2019, pp. 36-42, (doi: 10.1016/j.compscitech.2018.12.030).

[7]   S. Somashekar, V. Manjunath, M. Gowtham, and N. Balasubramaniam, Investigation on Mechanical Properties of Hemp–E Glass Fiber Reinforced Polymer Composites, *International Journal of Mechanical Engineering and Technology*, **7**, 2016, pp. 182-192.

[8]   M.A. Abd El-Baky, M.A. Attia, M.M. Abdelhaleem, and M.A. Hassan, Flax/basalt/E-glass Fibers Reinforced Epoxy Composites with Enhanced Mechanical Properties, *Journal of Natural Fibers*, **19**, 2022, pp. 954-968, (doi: 10.1080/15440478.2020.1775750).

[9]   G. Kalaprasad *et al.*, Effect of fibre length and chemical modifications on the tensile properties of intimately mixed short sisal/glass hybrid fibre reinforced low density polyethylene composites, *Polymer International*, **53**, 2004, pp. 1624-1638, (doi: 10.1002/pi.1453).

[10]   G.R. Arpitha, M.R. Sanjay, P. Senthamaraikannan, C. Barile, and B. Yogesha, Hybridization Effect of Sisal/Glass/Epoxy/Filler Based Woven Fabric Reinforced Composites, *Experimental Techniques*, **41**, 2017, pp. 577-584, (doi: 10.1007/s40799-017-0203-4).

[11]   V. Fiore, G. Di Bella, and A. Valenza, Glass–basalt/epoxy hybrid composites for marine applications, *Materials & Design*, **32**, 2011, pp. 2091-2099, (doi: 10.1016/j.matdes.2010.11.043).

[12]   N. Patel, K. Patel, P. Gohil, and V. Chaudhry, Investigations on mechanical strength of hybrid basalt/glass polyester composites, *Int. J. Appl. Eng. Res*, **13**, 2018, pp. 4083-4088.

[13]   S.M. Sapuan *et al.*, Mechanical Properties of Longitudinal Basalt/Woven-Glass-Fiber-reinforced Unsaturated Polyester-Resin Hybrid Composites, *Polymers*, **12**, 2020, p. 2211, (doi: 10.3390/polym12102211).

[14]   M.Y. Khalid, Z.U. Arif, M.F. Sheikh, and M.A. Nasir, Mechanical characterization of glass and jute fiber-based hybrid composites fabricated through compression molding technique, *International Journal of Material Forming*, **14**, 2021, pp. 1085-1095, (doi: 10.1007/s12289-021-01624-w).

[15]   A. Prashanth, D. Suresh, and E.V. Reddy, Experimental Investigation of Hybrid Hemp-Glass Fiber Reinforced Epoxy Composite, *International Journal of Innovative Research & Studies*, **8**, 2018, pp. 416-423.

[16]   M.A. Abd El-baky, M.A. Attia, M.M. Abdelhaleem, and M.A. Hassan, Mechanical characterization of hybrid composites based on flax, basalt and glass fibers, *Journal of Composite Materials*, **54**, 2020, pp. 4185-4205, (doi: 10.1177/0021998320928509).

[17]   H. Dalfi, K.B. Katnam, and P. Potluri, Intra-laminar toughening mechanisms to enhance impact damage tolerance of 2D woven composite laminates via yarn-level fiber hybridization and fiber architecture, *Polymer Composites*, **40**, 2019, pp. 4573-4587, (doi: 10.1002/pc.25325).

[18]   P.J. Hogg, Toughening of thermosetting composites with thermoplastic fibres, *Materials Science and Engineering: A*, **412**, 2005, pp. 97-103, (doi: 10.1016/j.msea.2005.08.028).

[19]   E. Selver, P. Potluri, P. Hogg, and C. Soutis, Impact damage tolerance of thermoset composites reinforced with hybrid commingled yarns, *Compos Part B: Eng*, **91**, 2016, pp. 522-538, (doi: 10.1016/j.compositesb.2015.12.035).

[20]   K.B. Katnam, H. Dalfi, and P. Potluri, Towards balancing in-plane mechanical properties and impact damage tolerance of composite laminates using quasi-UD woven fabrics with hybrid warp yarns, *Composite Structures*, **225**, 2019, (doi: 10.1016/j.compstruct.2019.111083).

[21]   H. Dalfi, A.J. Al-Obaidi, and H. Razaq, The influence of the inter-ply hybridisation on the mechanical performance of composite laminates: Experimental and numerical analysis, *Science Progress*, **104**, 2021, p. 00368504211023285, (doi: 10.1177/00368504211023285).

[22]   M. Cao, Y. Zhao, B.H. Gu, B.Z. Sun, and T.E. Tay, Progressive failure of inter-woven carbon-Dyneema fabric reinforced hybrid composites, *Composite Structures*, **211**, 2019, pp. 175-186, (doi: 10.1016/j.compstruct.2018.12.024).

[23]   P. Priyanka, H.S. Mali, and A. Dixit, Mesoscale Numerical Characterization of Kevlar and Carbon–Kevlar Hybrid Plain-Woven Fabric Compression Behavior, *Journal of Materials Engineering and Performance*, **28**, 2019, pp. 5749-5762, (doi: 10.1007/s11665-019-04306-6).

[24] S. Banerjee and B.V. Sankar, Mechanical properties of hybrid composites using finite element method based micromechanics, *Compos Part B: Eng*, **58**, 2014, pp. 318-327, (doi: 10.1016/j.compositesb.2013.10.065).

[25] E.A.W. de Menezes, F. Eggers, R.J. Marczak, I. Iturrioz, and S.C. Amico, Hybrid composites: Experimental, numerical and analytical assessment aided by online software, *Mech. Mater.*, **148**, 2020, p. 103533, (doi: h10.1016/j.mechmat.2020.103533).

[26] S. Nemat-Nasser and M. Hori, *Micromechanics: overall properties of heterogeneous materials*. Elsevier, 2013.

[27] Z. Xia, Y. Zhang, and F. Ellyin, A unified periodical boundary conditions for representative volume elements of composites and applications, *Int. J. Solids Struct.*, **40**, 2003, pp. 1907-1921, (doi: 10.1016/s0020-7683(03)00024-6).

[28] L. Yang, Y. Yan, Z. Ran, and Y. Liu, A new method for generating random fibre distributions for fibre reinforced composites, *Composites Science and Technology*, **76**, 2013, pp. 14-20, (doi: 10.1016/j.compscitech.2012.12.001).

[29] D. Scida, Z. Aboura, M.L. Benzeggagh, and E. Bocherens, A micromechanics model for 3D elasticity and failure of woven-fibre composite materials, *Composites Science and Technology*, **59**, 1999, pp. 505-517, (doi: 10.1016/S0266-3538(98)00096-7).

[30] Huntsman. Advanced Materials Araldite® LY 564* / Aradur® 2954*

[31] P. Valentino, M. Romano, I. Ehrlich, F. Furgiuele, and N. Gebbeken, Mechanical characterization of basalt fibre reinforced plastic with different fabric reinforcements – Tensile tests and FE-calculations with representative volume elements (RVEs), *Acta Fracturae - XXll Convegno Nazionale IGF (Italiano Gruppo Frattura) (Eds. F. Iacovello, G. Risitano, and L. Susmel)*, *Roma*, *July 1-3 2013*, Gruppo Italiano Frattura, pp. 231-237.

[32] Y. Zhong, L.Q.N. Tran, U. Kureemun, and H.P. Lee, Prediction of the mechanical behavior of flax polypropylene composites based on multi-scale finite element analysis, *Journal of Materials Science*, **52**, 2017, pp. 4957-4967, (doi: 10.1007/s10853-016-0733-7).

[33] V. Chauhan, T. Kärki, and J. Varis, Review of natural fiber-reinforced engineering plastic composites, their applications in the transportation sector and processing techniques, *Journal of Thermoplastic Composite Materials*, **35**, 2019, pp. 1169-1209, (doi: 10.1177/0892705719889095).

[34] G.S. Dhaliwal, S.M. Dueck, and G.M. Newaz, Experimental and numerical characterization of mechanical properties of hemp fiber reinforced composites using multiscale analysis approach, *SN Applied Sciences*, **1**, 2019, (doi: 10.1007/s42452-019-1383-6).

[35] S. Li and E. Sitnikova, *Representative Volume Elements and Unit Cells: Concepts, Theory, Applications and Implementation*. Woodhead Publishing, 2019.

[36] C.C. Chamis, Simplified composite micromechanics equations for hygral, thermal and mechanical properties., *SAMPE Quarterly*,1984, pp. 14-23.

[37] J.C.H. Affdl and J.L. Kardos, The Halpin-Tsai equations: A review, *Polymer Engineering & Science*, **16**, 1976, pp. 344-352, (doi: 10.1002/pen.760160512).

[38] T. Mori and K. Tanaka, Average stress in matrix and average elastic energy of materials with misfitting inclusions, *Acta Metallurgica*, **21**, 1973, pp. 571-574, (doi: 10.1016/0001-6160(73)90064-3).